A LEED study of NO superstructures on the Pd(111) surface

2009 J. Phys.: Condens. Matter 21 134005

(http://iopscience.iop.org/0953-8984/21/13/134005)

J. Phys.: Condens. Matter **21** (2009) 134005 (7pp) doi:10.1088/0953-8984/21/13/134005

A LEED study of NO superstructures on the Pd(111) surface

Petr Kostelník[1,3], Tomáš Šikola[1], Peter Varga[2] and Michael Schmid[2]

[1] Institute of Physical Engineering, Brno University of Technology, 61669 Brno, Czech Republic
[2] Institut für Allgemeine Physik, Technische Universität Wien, A-1040 Wien, Austria

E-mail: schmid@iap.tuwien.ac.at

Received 16 October 2008, in final form 21 November 2008
Published 12 March 2009
Online at stacks.iop.org/JPhysCM/21/134005

Abstract
We have examined two adsorption structures of NO on the Pd(111) surface and the transformation between them. Low-energy electron diffraction (LEED) $I(V)$ curves of the Pd(111)–p(2 × 2)-NO and Pd(111)–c(4 × 2)-NO surface structures were acquired and analyzed using tensor LEED. Our structural models confirm a previous study by scanning tunneling microscopy and DFT (Hansen *et al* 2002 *Surf. Sci.* **496** 1). In the c(4 × 2)-NO structure, which forms at an NO coverage of 0.5 monolayers (ML), the NO molecules occupy fcc and hcp hollow sites and are almost upright with only slight tilting, possibly related to NO–NO repulsion. In the p(2 × 2)-NO structure (0.75 ML), with two NO molecules in hollow sites and one in an on-top site, we find strong tilting of the on-top molecule. Upon heating, thermal desorption of NO leads to a transition from the p(2 × 2) to the c(4 × 2) structure, which leads to splitting of the diffraction spots and/or streaky spots. The transition is discussed in terms of domain walls.

1. Introduction

Surface structures of transition metals have been the object of intensive studies for a long time due to their use for catalytic reactions, e.g. for exhaust gas treatment [1]. One of these reactions is the catalytic reduction of NO to N_2 and O_2. NO adsorption on transition metals is known to occur in both molecular and dissociative ways [2, 3].

There are four different adsorption structures of NO on the Pd(111) surface for adsorption temperatures in the range of 100–300 K [5]. The first three structures are associated with three different peaks in temperature-dependent desorption (α, β and γ) [6]. The α peak is associated with the occurrence of the p(2 × 2) structure at an NO coverage of 3/4 ML and the β peak is associated with the c(4 × 2) structure at an NO coverage of 1/2 ML. The γ peak is not associated with any long-range structure and exists at a coverage of 1/4 ML. Chen *et al* [4] and Hansen *et al* [5] reported also a c(8 × 2) structure at a coverage of 5/8 ML. Hansen observed the c(8 × 2) only coexisting with the two other ordered structures, but never as a complete overlayer.

The p(2 × 2) and c(4 × 2) surface structures have been studied extensively in the past using various spectroscopy techniques [2, 4, 6], scanning tunneling microscopy [5] and density functional theory calculations (DFT) [5, 7, 8], but no classical surface crystallography methods such as quantitative low-energy electron diffraction (LEED) have been applied so far, possibly because problems with electron-stimulated desorption (ESD) of the NO molecules were expected. First models [2, 4] showed the NO molecules in the substrate bridge positions, the later ones [7, 8] in fcc and hcp hollow substrate sites as well as on top of substrate atoms. The latest DFT-based study of these structures [5] predicted that the on-top molecules should be tilted.

In the present paper, we report on the first quantitative LEED $I(V)$ study of the p(2 × 2) and c(4 × 2) NO structures on the Pd(111) surface. Furthermore, we present results on the transformation of the p(2 × 2) to the c(4 × 2) structure induced by thermal desorption of NO. Using a highly sensitive CCD camera and rather low primary electron currents, ESD did not pose a problem to the measurements.

[3] Present address: ON Semiconductor Czech Republic, R&D Europe, 1. máje 2230, Rožnov pod Radhoštěm 75661, Czech Republic.

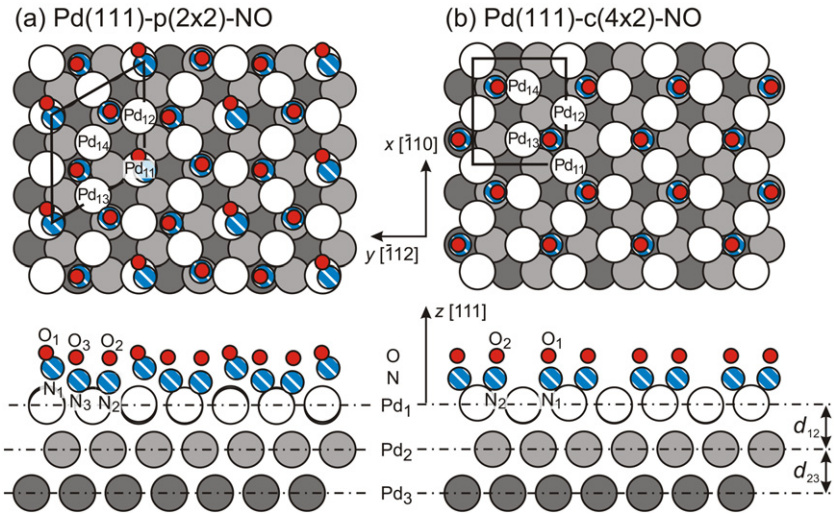

Figure 1. Models of the Pd(111)–p(2 × 2)-NO and Pd(111)–c(4 × 2)-NO surface structures based of the LEED results. (This figure is in colour only in the electronic version)

2. Experimental and computational details

The LEED experiments were performed in Vienna using commercial two-grid LEED optics (ErLEED) in a mu-metal UHV chamber with a base pressure in the 10^{-11} mbar range, which deteriorated to $\approx 3 \times 10^{-10}$ mbar during the series of experiments with NO. The sample holder in the chamber was equipped with a cooling system, reaching temperatures down to ≈100 K when cooling with liquid nitrogen.

A Pd(111) single crystal was used as a substrate. The crystal was cleaned by several cycles of sputtering by Ar^+ ions (500 eV, 2 μA, 30 min) and subsequent annealing by electron bombardment of the sample holder (900 K, 30 min). The cleanliness of the surface was examined by Auger electron spectroscopy (AES) using a cylindrical mirror analyzer with coaxial electron source. There was no contamination by the usual impurities (C, O, S) visible in the AES spectra after cleaning and only a sharp diffraction pattern of the (111) surface was visible on the LEED diffraction screen.

The LEED $I(V)$ measurements were performed at normal incidence of the electron beam. The LEED patterns for both p(2 × 2) and c(4 × 2) structures starting from 50 up to 350 eV in 2 eV steps were recorded and stored for further analysis. We have used a highly sensitive video camera (Watec 120N), allowing us to use a low electron current (<1 μA) in the LEED experiments. The symmetrically equivalent $I(V)$ curves were averaged, smoothed and normalized to the primary electron current, giving a set of 17 symmetrically inequivalent $I(V)$ curves (5 integer and 12 fractional) with a total energy range of 3092 eV for the p(2 × 2) and a set of 20 symmetrically inequivalent curves (5 integer and 15 fractional) with an energy range of 4522 eV for the c(4 × 2) structure. Overall intensities of the diffraction patterns were recorded before and after the experiments to determine any changes in quality of the structure. We did not find any changes; thus the sample was not damaged by ESD.

The University of Erlangen TensErLEED program package [9] was used for calculating $I(V)$ curves and searching for the optimum structures. The package uses standard dynamical theory of diffraction and the tensor LEED [10] perturbation method as well. Phase shifts for palladium, oxygen and nitrogen were calculated using a program by van Hove [11], for simplicity only using bulk parameters. The phase shift cutoff was $l \leqslant 9$.

Optimization was done for all atomic coordinates in the NO molecules. We did not impose any symmetry constraints on the N and O atoms, allowing them to take any arbitrary tilt and in-plane position within the range searched. As NO does not bind very strongly to the Pd surface, we can assume only weak relaxations of the Pd substrate. Therefore, we have only varied the individual vertical coordinates of the Pd atoms in the uppermost Pd layer (Pd_1; see figure 1). For the p(2 × 2) structure, the second Pd layer was rigidly shifted in the z direction, i.e. only the interlayer distances d_{12} and d_{23} were varied. In the case of the c(4 × 2) overlayer, the lower number of NO molecules and larger experimental database has allowed us to vary also the individual z coordinates of the Pd atoms in the second layer, in addition to the interlayer distances d_{12} and d_{23}.

Concerning the non-structural parameters, the real part of the inner potential was varied, starting from the value of $V_{0r} = -7.7$ eV found in our previous study of the Pd(100) surface [12]. The imaginary part of the inner potential was fixed at $V_{0i} = -5$ eV according to Saidy *et al* [13] during the whole calculation. As usual, the vibration amplitude values given in this work are root-mean-square values of the three-dimensional displacement vectors and also include static disorder that is not covered by the variation of the geometrical parameters. The vibration amplitudes of the bulk Pd atoms were set to 0.08 and 0.11 Å for the p(2 × 2) and c(4 × 2) structures, respectively, reflecting the different temperatures of the measurements (≈140 and ≈245 K) and the bulk Debye temperature of 274 K. The vibration amplitudes of the oxygen and nitrogen atoms were initially both set to 0.10 Å for the p(2 × 2) and 0.14 Å for the c(4 × 2) structure, and further

optimized for each chemical species, along with the vibration amplitudes of the upper two palladium layers.

This results in a total of 28 independent parameters with 110 eV range per free parameter for the p(2 × 2) structure and 25 independent parameters (180 eV per parameter) for the c(4 × 2) structure.

The search process consisted of refinement cycles with decreasing step size, alternating between refinement of the vertical and the in-plane NO coordinates. The vertical coordinates of Pd were varied in each optimization step. Each cycle consisted of a full dynamical reference calculation, a tensor LEED delta calculation and the search for the best-fit structure. For determining the agreement between experimental and theoretical $I(V)$ curves, Pendry's reliability factor R_p [14] was used.

3. Results and discussion

3.1. Preparation of the NO superstructures

The Pd(111)–p(2 × 2)-NO surface was prepared by exposure of the clean Pd(111) surface to NO at a temperature below 140 K. A pressure of 5×10^{-6} mbar was applied for 7 min, resulting in a total dose slightly above 1500 L (Langmuir; 1 L = 1.33×10^{-6} mbar s), enough to guarantee that the saturation coverage was reached. A sharp p(2 × 2) pattern was visible on the diffraction screen after the procedure; LEED $I(V)$ data were acquired at ≈140 K.

The Pd(111)–c(4 × 2) surface was prepared by heating of the p(2 × 2) surface. Upon heating from 140 K, the p(2 × 2) surface is stable until a temperature of 210 K is reached, then a transition to the c(4 × 2) structure follows (see section 3.3). At a temperature of 245 K, only the fully developed c(4 × 2) structure is observed. The c(4 × 2) structure starts to degrade at temperature of approximately 255 K, hence for the LEED $I(V)$ measurements the temperature had to be kept in the range of 210–255 K to ensure stability of the c(4 × 2) structure, while avoiding formation of the p(2 × 2) structure from the NO desorbing from the chamber walls.

3.2. Tensor LEED results

3.2.1. Pd(111)–p(2 × 2)-NO. The input for the tensor LEED $I(V)$ analysis was the model by Hansen *et al* [5], with NO molecules in the fcc and hcp hollow sites. As preliminary density functional theory (DFT) calculations [15] resulted in a tilt of the on-top NO molecule in a direction different from this model, towards the hcp site, not the fcc site, three separate models were tested by LEED. The first model had the NO molecule tilted towards the hcp site, the second model was without tilting of the on-top NO molecule and the third model had the on-top NO molecule rotated by 60° with respect to the first one, i.e. in the same direction as in Hansen's model.

We started with improving the first model. During the optimization the tilted on-top NO molecule was observed to rotate from the hcp to the fcc substrate site, i.e. towards the orientation of Hansen's model. The final model shows a tilting of 47° from the surface normal. This model turned out to have the best Pendry R factor of $R_p = 0.243$ of all three models and therefore is presented as the best-fit model. The resulting parameters are shown in table 1 and the experimental and calculated $I(V)$ curves are displayed in figure 2. Interestingly, the final positions of the on-top NO molecule and the Pd atom below are not exactly in one plane but the molecule appears shifted slightly sidewards (figure 1). Considering the rather large vibration amplitudes A_{vib} found, this may indicate an in-plane vibration amplitude that is larger than that perpendicular to the surface (the calculations are for isotropic vibrations only).

Table 1. Optimized parameters of the Pd(111)–p(2 × 2)-NO structure. Interlayer distances d_{ij} and relative z values Δz are given with respect to the center of mass of the respective Pd layer. The base vectors of the (2 × 2) cell are $\mathbf{a}_1 = (5.502, 0.000)$ Å and $\mathbf{a}_2 = (-2.751, 4.765)$ Å. The asterisk (∗) indicates values not varied in the LEED structural search.

Atom	x (Å)	y (Å)	Δz (Å)	A_{vib} (Å)
O_1	0.69	0.02	2.73	0.185
O_2	3.01	1.49	2.50	
O_3	−0.04	3.23	2.46	
N_1	−0.09	−0.32	1.94	0.175
N_2	2.95	1.54	1.29	
N_3	−0.05	3.08	1.20	
Pd_{11}	0.000*	0.000*	0.07	0.15
Pd_{12}	2.751*	0.000*	−0.03	
Pd_{13}	−1.376*	2.383*	−0.04	
Pd_{14}	1.376*	2.383*	0.00	
d_{12}			2.31	
Pd_{2n}				0.12
d_{23}			2.26	

In the case of the second model optimization, all computational settings were the same as for the first one except for the horizontal optimization range of the nitrogen and oxygen atoms, which was initially set to ±0.4 Å, enabling the NO molecules to shift and tilt considerably from the upright position. The on-top NO molecule started to tilt during the search process, ending in tilting towards the hcp substrate site as seen in the preliminary DFT results mentioned above. This azimuthal orientation of the on-top NO molecule is the only difference between the resulting structures of the two models. The other parameters show excellent agreement. As the final R factor of the model with the NO molecule tilted towards the hcp site, $R_p = 0.276$ is significantly higher than that with tilting towards the fcc site and above the variance limit [14] of 0.271, this result cannot be considered the best-fit model and must be attributed to a local minimum.

For the third model with the NO molecule tilted already as in Hansen's model, a search with the same procedure as for the first model did not lead to large changes of the coordinates of the on-top NO. As for model 1, the molecule's final position showed a slight shift against the exact on-top site. The structural search was terminated at an R factor of $R_p = 0.250$, almost the same as for the best-fit structure, with very small differences of the coordinates (lower than 0.08 Å).

3.2.2. Pd(111)–c(4 × 2)-NO. The reference structure for the tensor LEED $I(V)$ analysis was based on the structure presented previously [5], with the initial coordinates taken

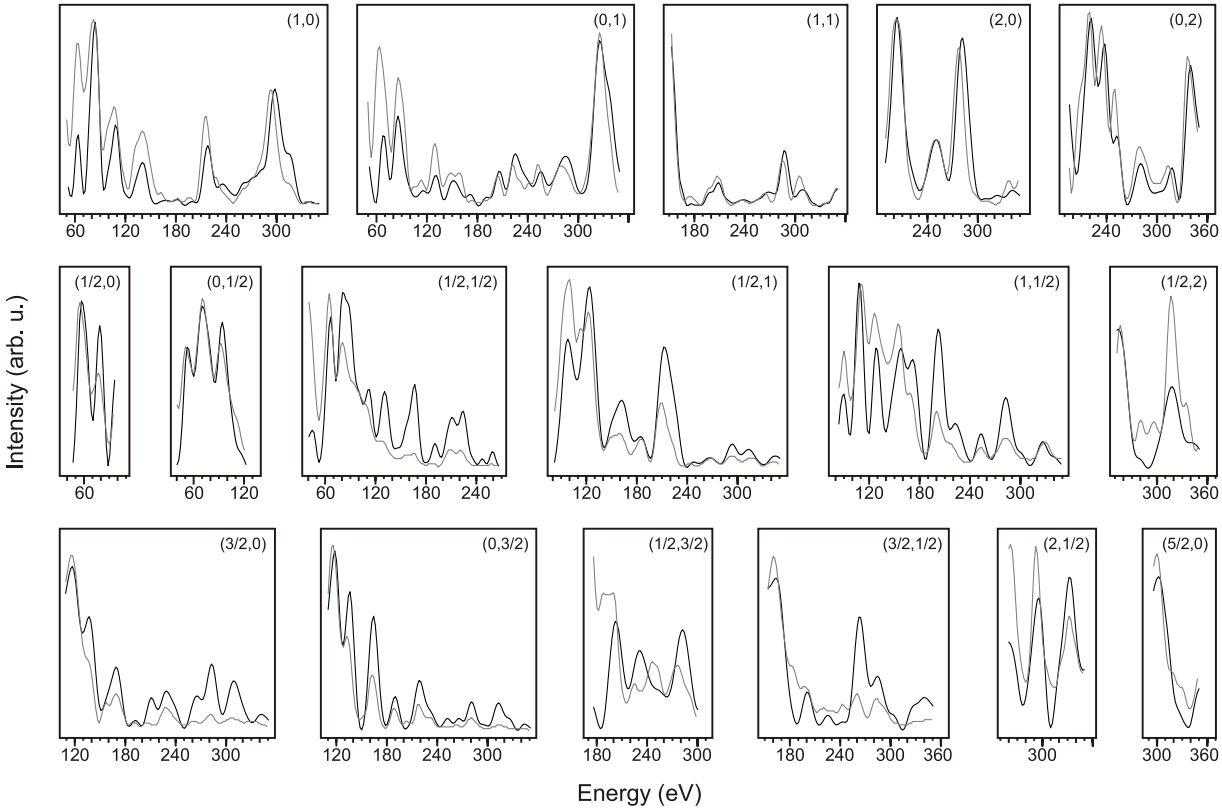

Figure 2. Comparison of the measured (black) and calculated (gray) $I(V)$ curves of the best-fit model for the Pd(111)–p(2 × 2)-NO surface structure ($R_p = 0.243$).

from preliminary DFT calculations [15]. The basis cell of our LEED calculations was not a c(4 × 2) cell but rather an equivalent rectangular one with side lengths of ($\sqrt{3} \times 2$), marked by a black rectangle in figure 1(b). The cell contains two NO molecules in the fcc and hcp substrate sites. As for the p(2 × 2) surface, we did not expect significant structural changes in the substrate and therefore only considered out-of-plane displacements of the Pd atoms, keeping their in-plane coordinates fixed. Initially, the coordinates were optimized independently within a range of ±0.2 Å from the reference position. Refinement finally resulted in a best-fit model of the c(4 × 2) structure (table 2) with a Pendry R factor of $R_p = 0.282$. This value may seem unsatisfactory at first glance, but the $I(V)$ curves shown in figure 3 demonstrate very good agreement between calculation and experiment. The deviations are mainly in ranges of low intensity. It should be also noted that the energy range per free parameter is exceptionally high in this case. While low-energy ranges per parameter may allow accommodating some noise or experimental artifacts by slight adjustment of the parameters, in the present case the overdetermination prevents such a reduction of the R factor.

Table 2. Optimized parameters of the Pd(111)–c(4 × 2)-NO structure. Interlayer distances d_{ij} and relative z values Δz are given with respect to the center of mass of the respective Pd layer. The base vectors of the c($\sqrt{3} \times 2$)$_{rect}$ cell are $\mathbf{a}_1 = (5.502, 0.000)$ Å and $\mathbf{a}_2 = (0.000, 4.765)$ Å. The asterisk (∗) indicates values not varied in the LEED structural search.

Atom	x (Å)	y (Å)	Δz (Å)	A_{vib} (Å)
O_1	1.27	1.05	2.45	0.195
O_2	4.26	3.70	2.49	
N_1	1.33	0.90	1.24	0.155
N_2	4.11	3.80	1.27	
Pd_{11}	0.000*	0.000*	0.02	0.14
Pd_{12}	2.751*	0.000*	0.10	
Pd_{13}	1.376*	2.383*	−0.06	
Pd_{14}	4.127*	2.383*	−0.06	
d_{12}			2.30	
Pd_{21}	−1.376*	−0.794*	−0.00	0.13
Pd_{22}	1.376*	−0.794*	0.02	
Pd_{23}	0.000*	1.588*	−0.00	
Pd_{24}	2.751*	1.588*	−0.02	
d_{23}			2.27	

3.3. The p(2 × 2) to c(4 × 2) transition

As mentioned above, the transition from the p(2 × 2) to the c(4 × 2) structure takes place between 210 K, where the p(2 × 2) diffraction pattern starts to degrade, and 245 K, where the c(4 × 2) structure appears with sharp spots. While re-cooling the sample from the upper stability limit of the c(4 × 2) structure, from 255 to 130 K, we found that the c(4 × 2) is stable to 210 K. Further cooling brings back the p(2 × 2) structure, probably by adsorption of NO molecules desorbing from the UHV chamber walls.

The diffraction pattern of the p(2 × 2) structure (figure 4(a)) shows that the fractional spots are slightly elongated already in the otherwise perfect structure observed at

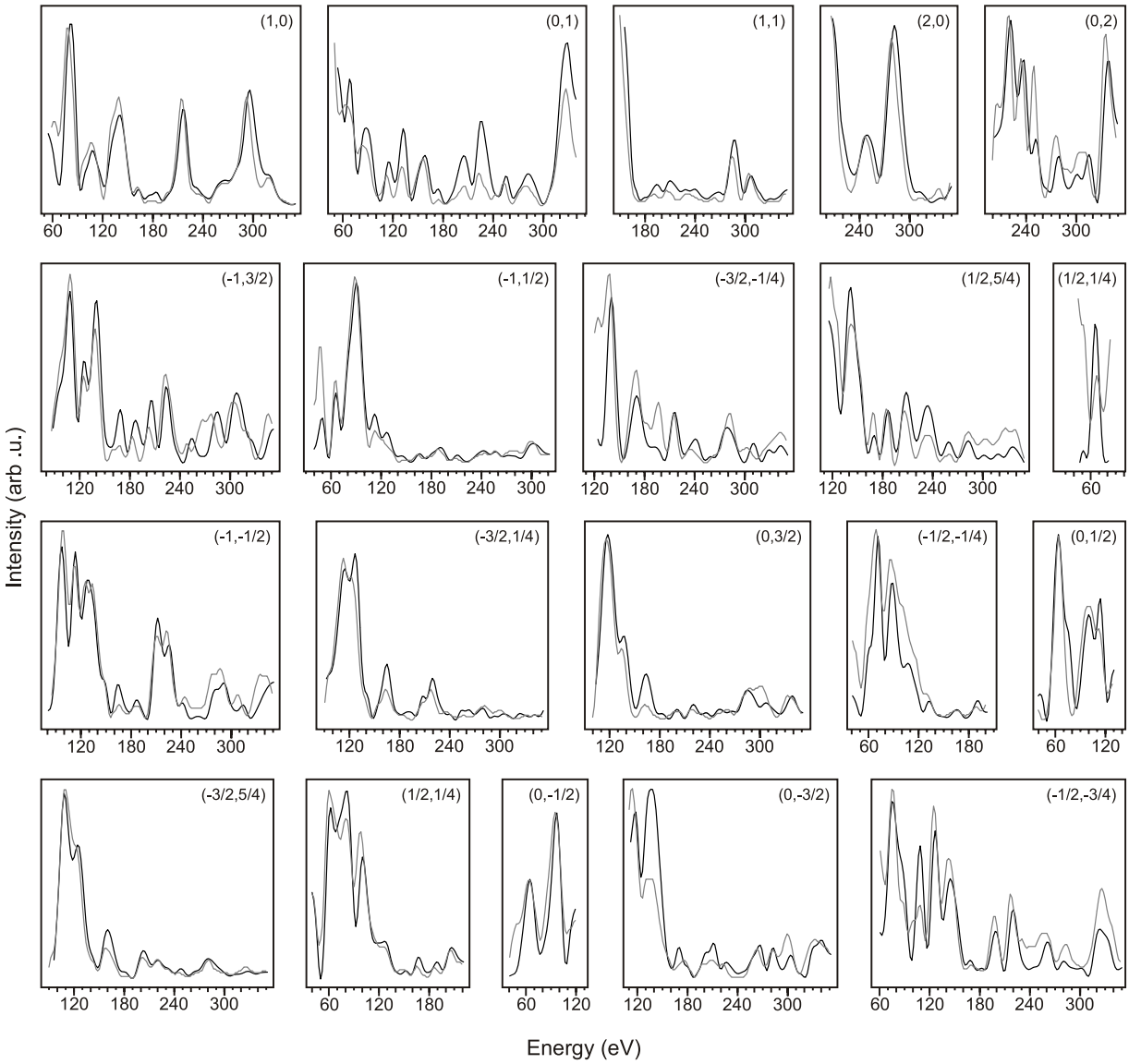

Figure 3. Comparison of the measured (black) and calculated (gray) $I(V)$ curves of the best-fit model of the Pd(111)–c(4 × 2)-NO surface structure ($R_p = 0.282$).

210 K (inset in figure 4(a)). With increasing temperature, i.e. decreasing NO coverage, the (1/2, 0) spots develop a bow-tie shape (figures 4(c) and (d)). The diffraction pattern observed at a temperature of 232 K (figure 4(d)) is a blurry c(8 × 2) pattern. This structure has been described previously [5] and is shown schematically in figure 4(e). Based on this model, we can explain the bow-tie pattern observed at lower temperatures by 'light' (i.e., NO-poor) domain walls in the p(2 × 2) structure, as indicated by the dashed line in figure 4(b). In the domain walls, the local arrangement of the NO molecules is the same as in the c(4 × 2) structure. Due to the repulsive interaction between the hcp-site and fcc-site NO molecules on the two sides of the domain wall, adjacent p(2 × 2) domains are displaced by $1/2[\bar{1}10]$, i.e. parallel to the domain wall (see the dotted lines in figure 4(b)). This explains why the fractional-order spots are not split or elongated in the radial direction but rather at an angle, as indicated by the double arrows 's' in figure 4(f). Two of the three different rotational orientations of the domain walls contribute to the corners of the bow-tie shape, while the third one has its spots in the center of the bow-tie (figure 4(f)).

With a further increase of the temperature, again leading to NO desorption, at a temperature of 239 K the diffraction pattern starts to resemble that of the c(4 × 2) structure (figure 4(g)). The diffuse intensity moves further in the directions of the arrows 's' in figure 4(f) and finally condenses into sharp (1/2, 1/4) spots when the c(4 × 2) structure is fully developed (figure 4(i)). This means that the structure continues to develop as before, with fewer and fewer rows of on-top NO molecules as the temperature increases. Figure 4(h) shows such a structure, where the spacing between the on-top NO rows corresponds to a p(8 × 2) periodicity. We can describe this model as a c(4 × 2) structure with 'heavy' domain walls formed by the additional rows of on-top NO. As the fuzziness of the LEED spots indicates, the domain walls are not equidistant, however, and no long-range order of the intermediate superstructures develops at these temperatures.

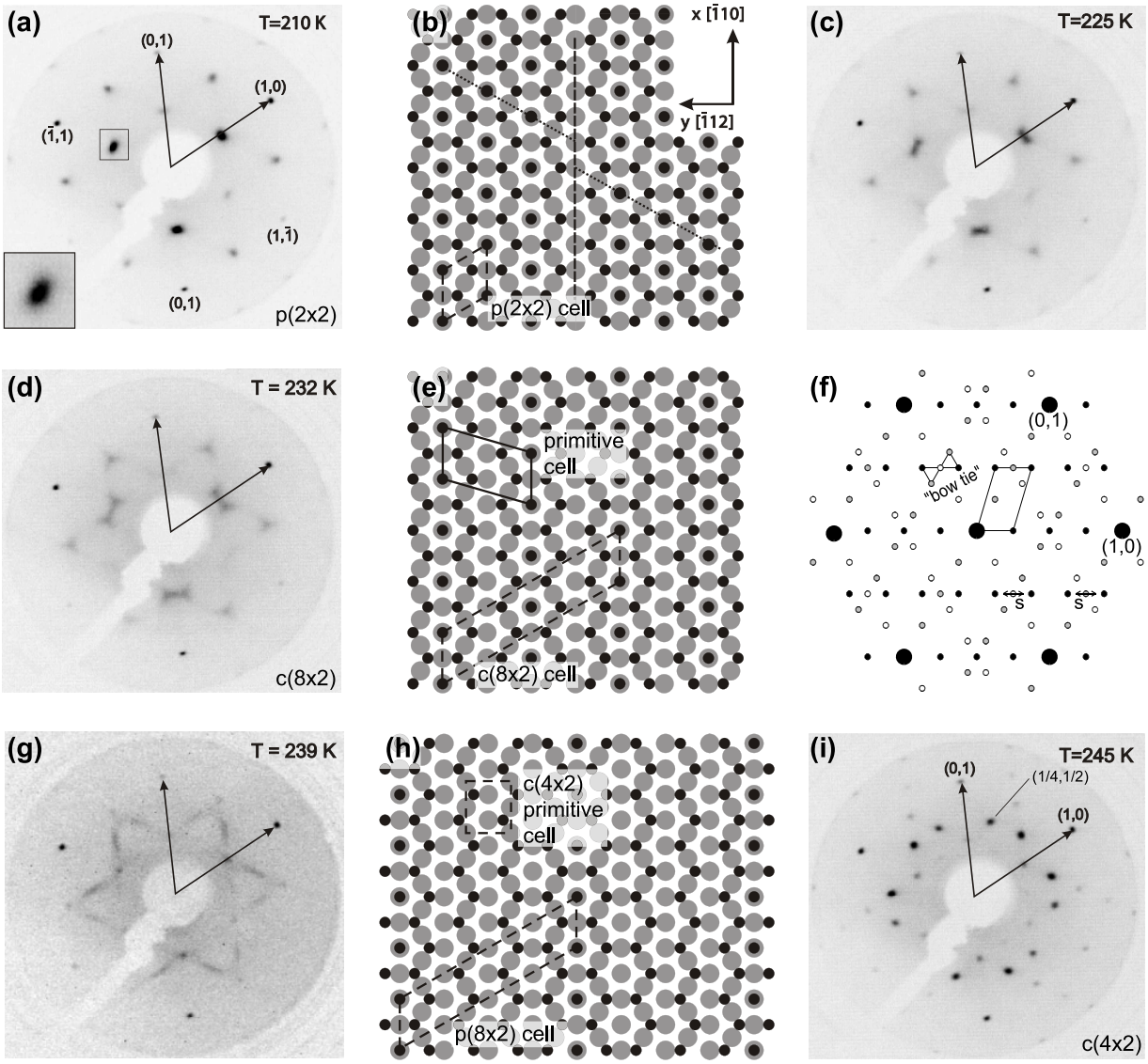

Figure 4. Transition between the p(2 × 2) and the c(4 × 2) structures with increasing temperature. (a) LEED diffraction pattern of the p(2 × 2) structure. (b) Model of the Pd(111)–p(2 × 2)-NO surface (palladium atoms are gray, NO molecules black) showing a domain wall, where a row of on-top NO molecules is absent (dashed). (c), (d) Diffraction patterns showing the development of the bow-tie shape of the fractional spots towards the c(8 × 2) structure. (e) Schematics of the c(8 × 2) structure and (f) the c(8 × 2) diffraction pattern with the three rotational domains marked by filled (black), gray and open circles. (g) Diffraction pattern at 239 K showing the transition towards the c(4 × 2) structure. (h) Schematics of the c(4 × 2) structure with additional rows of on-top NO molecules, forming a p(8 × 2) structure. (i) Diffraction pattern of the c(4 × 2) structure. All diffractions patterns at $E = 80$ eV.

3.4. Discussion

As we did not perform the tedious task of trying out all the different structural models conceivable, our results do not directly rule out adsorption geometries different from those proposed in the previous STM/DFT study [5] and also found by us. The good agreement of the experimental and calculated $I(V)$ curves (figures 2 and 3) over a very high range of energy, especially when compared to the number of free parameters, strongly suggests that the models are correct, however. Furthermore, the search algorithm employed [16], starting from different initial configurations in each search run, and also the lack of any symmetry constraint for the N and O coordinates makes it very unlikely to end up in a local minimum of the R factor, giving the wrong structure. The strongest argument comes from the bonding geometry observed in our models: Fitting to a wrong structural model usually results in unphysical bond lengths; in our models the bond lengths and also the other structural parameters are all reasonable and show the expected trends. Furthermore, the coordinates of symmetry-equivalent atoms, which were unconstrained in the calculation, show good agreement with the symmetries expected; the only exception being the slight sideward movements of the NO molecules in the c(4 × 2) structure mentioned earlier. (For the p(2 × 2) structure, the full symmetry of a centered rectangular cell with its long axis parallel to the azimuthal direction of the on-top NO is $c1m1$; the rectangular cell of the c(4 × 2) structure has $p2gg$ symmetry.)

Table 3. Bond lengths d and tilting angles θ of the NO molecules in the Pd(111)–p(2 × 2)-NO and Pd(111)–c(4 × 2)-NO structures.

Structure/atoms	d (Å)	θ (deg)
p(2 × 2)–NO		
N_1–O_1	1.16	47
N_2–O_2	1.21	4
N_3–O_3	1.27	7
N_1–Pd_{11}	1.86	
N_2–$Pd_{12,13,14}$	2.04, 1.97, 2.20	
N_3–$Pd_{12,13,14}$	2.09, 1.94, 1.99	
c(4 × 2)–NO		
N_1–O_1	1.22	8
N_2–O_2	1.23	8
N_1–$Pd_{11,12,13}$	2.02, 2.03, 1.97	
N_2–$Pd_{11,12,14}$	2.08, 2.04, 1.94	

The N–O bond lengths in our models (table 3), lying between 1.16 and 1.27 Å, agree well with other determinations, e.g. for NO on Pt(111), where bond lengths of 1.19 and around 1.20–1.21 Å have been found in LEED [17] and x-ray absorption studies [18], respectively. The Pd–N bond lengths of the NO molecules in hollow sites are all around 2 Å, the same range as found in a previous LEED study of NO/Pt(111), where d_{N-Pt} distances in the range of 2.01–2.12 Å were found [17]. The Pd–N bond length for the on-top NO molecule is shorter, in agreement with the trend of decreasing bond length (increasing bond strength) with decreasing coordination.

As predicted by DFT, the on-top NO molecule is strongly tilted; the tilting angle of 47° agrees well with the value of 40° determined by DFT [5]. We also find a slight tilting of the hollow-site NO molecules. At least in the c(4 × 2) structure we consider this a real effect as both NO molecules show exactly the same tilting angle and the tilt is in the direction expected for a repulsion between the NO molecules. This tilting is accompanied by a shorter bond length of the N atoms to the Pd atom having the lower coordination (Pd_{13} or Pd_{14}). These observations are analogous to the structurally equivalent Ni(111)–c(4 × 2) NO surface [19].

Concerning the vertical relaxations of the Pd surface atoms, the usual trend can be observed: stronger bonding to adsorbates moves the Pd atoms outwards. In the p(2 × 2) structure, the Pd atom below the on-top NO relaxes outwards by 0.07 Å with respect to the center of mass of the layer (0.13 Å with respect to the bulk interlayer distance). The three other Pd atoms have to share two NO molecules, resulting in lower relaxations. In the c(4 × 2) structure, the Pd_{11} and Pd_{12} atoms have a higher coordination to NO than Pd_{13} and Pd_{14}, thus the first are higher in z than the latter. The height of the Pd_{13} and Pd_{14} atoms above the Pd_2 layer is exactly equal to the bulk interlayer spacing of Pd. It is interesting, however, that previous LEED studies [20, 21] found about 2% outwards relaxation for the first layer of the clean Pd(111) surface; this should let us expect an even more pronounced outwards relaxation of the Pd atoms here, since they all bind to NO. The question of the relaxation of the clean Pd(111) surface is not settled, however, since *ab initio* calculations usually predict an inwards relaxation [22].

4. Conclusions

We have analyzed the p(2 × 2) and c(4 × 2) NO adsorption structures on the Pd(111) surface by quantitative LEED. Our results agree with the previously proposed DFT-based models of these surface structures and we confirm the strong tilting of the on-top NO molecules predicted by DFT. We have also presented an explanation of the p(2 × 2) to c(4 × 2) transition in terms of creation of domain walls.

Acknowledgments

We would like to thank Miroslav Čák for preliminary DFT calculations serving as the starting point for the structural search by LEED. The project was supported by the Ministry of Education CR grant no. LC06040, the GACR grant no. FON06/E001 and by the Austrian *Fonds zur Förderung der wissenschaftlichen Forschung*.

References

[1] Farrauto R J and Heck R M 1999 *Catal. Today* **51** 351
[2] Bertolo M and Jacobi K 1990 *Surf. Sci.* **226** 207
[3] Brown W A and King D A 2000 *J. Phys. Chem.* B **104** 2578
[4] Chen P J and Goodman D W 1993 *Surf. Sci. Lett.* **297** L93
[5] Hansen K H, Šljivančanin Ž, Hammer B, Lægsgaard E, Besenbacher F and Stensgaard I 2002 *Surf. Sci.* **496** 1
[6] Conrad H, Ertl G, Küppers J and Latta E E 1977 *Surf. Sci.* **65** 235
[7] Loffreda D, Simon D and Sautet P 1998 *Chem. Phys. Lett.* **291** 15
[8] Loffreda D, Simon D and Sautet P 1998 *J. Chem. Phys.* **108** 6447
[9] Blum V and Heinz K 2001 *Comput. Phys. Commun.* **134** 392
[10] Rous R J and Pendry J B 1989 *Surf. Sci.* **219** 355
[11] Barbieri A and Van Hove M A, private communication
[12] Kostelník P, Seriani N, Kresse G, Mikkelsen A, Lundgren E, Blum V, Šikola T, Varga P and Schmid M 2007 *Surf. Sci.* **601** 1574
[13] Saidy M, Warren O L, Thiel P A and Mitchell K A R 2001 *Surf. Sci.* **494** L799
[14] Pendry J B 1980 *J. Phys. C: Solid State Phys.* **13** 937
[15] Čák M, private communication
[16] Kottcke M and Heinz K 1997 *Surf. Sci.* **376** 352
[17] Matsumoto M, Tatsumi N, Fukutani K and Okano T 2002 *Surf. Sci.* **513** 485
[18] Zhu P, Shimada T, Kondoh H, Nakai I, Nagasaka M and Ohta T 2004 *Surf. Sci.* **565** 232
[19] Materer N, Barbieri A, Gardin D, Starke U, Batteas J D, Van Hove M A and Somorjai G A 1994 *Surf. Sci.* **303** 319
[20] Barbieri A, Van Hove M A and Somorjai G A 1994 *Surf. Sci.* **306** 261
[21] Grillo M E, Stampfl C and Berndt W 1994 *Surf. Sci.* **317** 84
[22] Da Silva J L F, Stampfl C and Scheffler M 2006 *Surf. Sci.* **600** 703